Ceramics-Silikáty 69 (1), 63-74 (2025)
www.ceramics-silikaty.cz doi: 10.13168/cs.2024.0066

THE INFLUENCE OF THE MAGNESIUM ADDITIVE CONCENTRATION ON THE SYNTHESIS OF SILICON CARBIDE FROM RICE HUSKS

#KIEU DO TRUNG KIEN*, **, NGUYEN VU UYEN NHI*,**

*Ho Chi Minh City University of Technology (HCMUT), 268 Ly Thuong Kiet street, District 10, Ho Chi Minh City, Vietnam
**Vietnam National University Ho Chi Minh City, Linh Trung Ward, Thu Duc City, Ho Chi Minh City, Vietnam

#E-mail: kieudotrungkien@hcmut.edu.vn

Submitted September 22, 2024; accepted October 25, 2024

Keywords: Silicon carbide, Rice husks, Pyrolysis, Biomass

Silicon carbide is a compound known for its excellent wear resistance, thermal conductivity, and high-temperature stability. A key focus in the current SiC synthesis research is concerned with using biomass as a precursor. Rice husks represent a typical biomass material employed in producing SiC, though the conversion efficiency is often suboptimal. This study investigates the influence of magnesium additives on enhancing the SiC formation from rice husks. A mixture of rice husks, silica gel, and magnesium in various ratios was sintered at 1000 °C in a CO_2 atmosphere to synthesise SiC. The chemical composition, mineral phases, and microstructure analysis indicated that a rice husk-to-magnesium ratio of 1:6 was optimal for improving SiC yield. However, the additives also introduced unwanted impurities, which could be effectively removed through washing with hydrofluoric (HF) acid. After this purification step, the SiC content reached 84.25 % by weight. The final product exhibited both α-SiC and β-SiC allotropic forms, contributing to its enhanced mechanical strength and thermal stability.

INTRODUCTION

Vietnam is an agricultural nation with a significant rice production industry, generating a total rice output of 43.5 million tonnes annually. Of this, 8.3 million tonnes are exported, contributing 4.78 billion USD in revenue. Rice husks, a by-product of rice production, are commonly regarded as agricultural waste. In Vietnam, rice husks are primarily disposed of by burning, used as animal feed or fuel, or released directly into the environment [1]. Consequently, effectively utilising this waste material is a critical issue that requires attention. Many countries are now exploring ways to repurpose rice husks. These materials have been employed in producing various technical materials, including semiconductor components, industrial electronics, and aerospace materials [2-4]. Notably, rice husks can serve as a precursor for synthesising silicon carbide (SiC), a material with numerous advantageous properties [5].

SiC is a compound formed by the covalent bonding of carbon and silicon. Its crystal lattice structure resembles a diamond's, resulting in excellent mechanical strength and thermal resistance [6]. As a result, SiC is widely used in various applications, including furnace components, bearings, cutting tools, and in the semiconductor and aerospace industries. SiC is typically synthesised at high temperatures, usually exceeding 2000 °C [7]. Using natural raw materials and the high sintering temperatures lead to significant energy consumption, making SiC production challenging and costly. To address this issue, biomass materials have been explored as alternative sources for SiC synthesis [8], with rice husks being a commonly used feedstock [9]. As previously mentioned, rice husks contain carbon and silica, providing a large contact area that facilitates SiC formation at lower temperatures than usual [10]. However, the conversion efficiency for producing SiC is often low. Consequently, numerous studies have focused on enhancing the SiC yields by incorporating various additives.

Research findings have shown that additives can diminish the carbon and silica crystallisation in rice husks, thereby enhancing the formation of SiC [11]. F. N. Romero et al. compared the SiC synthesis from rice husks, evaluating the processes with and without the incorporation of additives. The findings demonstrated that additives significantly increased the reaction rate, yielding three times the output compared to the reaction without the additives. Other studies have utilised additives such as $FeCl_2$ or $FeSO_4$ to promote the SiC formation process [7, 12]. The results indicated that these two additives reduce the reaction temperature necessary for synthesising SiC. Furthermore, it was observed that the reaction rate is directly proportional to the surface area of the additives.

Various metal additives have been employed in studies on SiC synthesis in different research directions. Y. Shi et al. utilised magnesium as an additive to synthesise SiC [13]. SiC was successfully formed at 600 °C by reducing SiO2 to silicon via a reaction with Mg, followed by the reaction of Si with C to produce SiC. In addition to Mg, other metal additives such as iron, cobalt, and nickel have also been investigated to enhance the SiC production efficiency. F. J. N. Romero et al. [14] demonstrated that metal additives significantly improve the performance of the SiC synthesis. These metal additives help reduce the concentration of CO, a gas generated during the pyrolysis of a biomass, which can hinder the SiC formation. Consequently, this leads to an increase in the conversion efficiency of SiC from biomass feedstocks.

The studies above have indicated that using metal additives is an effective method for enhancing the SiC synthesis efficiency. Metals facilitate the early formation of a liquid phase, and the surface tension of this liquid phase improves the contact between the silicon and carbon particles. As a result, the reaction efficiency for the SiC formation increases. However, limited research has investigated the impact of metal additive concentrations on the SiC formation. This study examined concentrations of a magnesium additive to evaluate its effect on the SiC synthesis capability. The optimal Mg content was identified through a component analysis of SiC, X-ray diffraction, scanning electron microscopy, and energy-dispersive X-ray spectroscopy. The results also indicated that while the additive enhances the SiC production efficiency, it also leads to the formation of various impurities in the final product. Nevertheless, acid-washing techniques can remove these impurities from the additives.

EXPERIMENTAL

Materials

This study's primary rice husk (RH) materials were sourced from Vietnam's Mekong Delta region, ensuring a consistent and high-quality supply. The silica gel (SG) employed was synthesised through a chemical reaction involving liquid glass and acetic acid, as described by V. H. Le et al. [15]. This synthesis method was chosen to ensure the production of a highly reactive silica gel. The RHs contains 6.71 % SiO_2, 0.8 % R_2O, and 92.13 % loss on ignition (L.O.I) by weight. The silica gel has a composition of 67.83 % SiO_2, 1.38 % R_2O, and 30.37 % L.O.I by weight. Here, R_2O represents the combined weight percentage of K_2O and Na_2O. During sintering, the rice husks underwent thermal decomposition to produce activated carbon and silicon dioxide (SiO_2). Concurrently, the silica gel provided an additional source of activated SiO_2. The synergistic interaction between the activated carbon derived from the rice husks and the activated SiO_2 from the rice husks and the silica gel was pivotal in promoting the efficient formation of silicon carbide (SiC). This interaction facilitated the chemical reactions and phase transformations required for the SiC synthesis.

The magnesium (Mg) used in the experiments was commercial-grade, boasting a purity level greater than 99 %. This high-purity magnesium was procured from Merck. The purity of the magnesium was critical in minimising the impurities.

Procedure

Fine powdered rice husks and silica gel were employed in this study. The particle size analysis was performed using laser diffraction with a Horiba LA-920 model, yielding average particle sizes of 13.12 μm for the rice husks and 14.93 μm for the silica gel. The chemical compositions of the raw materials were determined via X-ray fluorescence (Thermo - ARL ADVANT'X).

The RH and SG were mixed in a weight ratio of 1/1.4. Magnesium was added as an additive in the weight ratios specified in Table 1. The mixed powders were subsequently subjected to sintering in a CO_2 atmosphere at 1000 °C. The CO_2 flow rate was controlled at 120 ml·min^{-1}, and the furnace heating rate was set to 10 °C·min^{-1}, with a soaking duration of 30 minutes. The sintering process was conducted in a tube furnace (model R170/750/13 from Nabertherm). The symbols used to represent the sintered samples are detailed in Table 1. The sintered samples underwent a hydrofluoric acid (HF) treatment, were neutralised with sodium hydroxide (NaOH), and then washed with distilled water. The experimental procedure is illustrated in Figure 1.

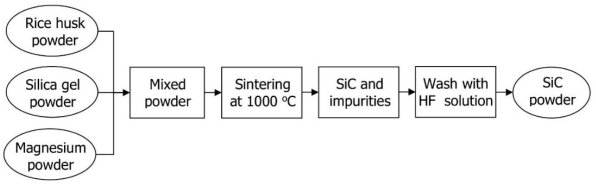

Figure 1. A diagram of the prototyping process.

Table 1. Details of the materials used in the study.

Samples	RH/SG (wt.)	RH/Mg (wt.)
Mg_0	1/1.4	1/0
Mg_2	1/1.4	1/2
Mg_4	1/1.4	1/4
Mg_6	1/1.4	1/6
Mg8	1/1.4	1/8

Analysis method

The compositions of silicon carbide (SiC), silicon dioxide (SiO_2), and carbon (C) in the samples were determined following the ISO 21068-2:2008 standard. This standard outlines a rigorous methodology for analysing these materials, ensuring precise and reliable SiC, SiO_2, and C quantification within the samples.

The phase composition was analysed using a Bruker D8 Advance X-ray diffraction (XRD) system. The XRD analysis was performed with Cu Kα radiation, having a wavelength (λ) of 0.154 nm. The powder samples were scanned over a 2θ range of 10° to 70°, with a step size of 0.019°, to achieve a detailed resolution of the diffraction patterns.

The microstructural examination and elemental distribution were conducted using Scanning Electron Microscopy (SEM) in conjunction with Energy Dispersive X-ray Spectroscopy (EDX). These analyses were performed with a JSM-IT 200 JEOL scanning electron microscope, which provided imaging and detailed elemental mapping of the sample surfaces.

RESULTS AND DISCUSSION

The sintered samples were analysed for their SiC content following the EN ISO 21068:2008 and EN 12698-1:2007 standards to evaluate the effect of the additive ratio on SiC formation. Figure 2 presents the results of the SiC content analysis for the samples sintered at 1000 °C.

The results of the SiC composition analysis show that the SiC content increases with the increase in the RH/Mg ratio from 1/0 to 1/6. The SiC content increases from 2.05 to 16.24 % by weight. These findings highlight the role of Mg additives in enhancing the efficiency of the SiC production. Previous studies suggest that Mg can promote increased contact between components by enhancing the diffusion of SiO onto the carbon surface, thereby improving the reaction efficiency between Si and C to form SiC. However, when the RH/Mg ratio increases to 1/8, the SiC content slightly decreases to 16.25 %. Molten Mg helps increase the component contact by rearranging particles due to surface tension effects, which can also hinder this contact. Excessive Mg may impair the reaction between the SiO gas in the calcination environment and amorphous carbon in the rice husks, leading to a slower SiC formation process and a subsequent reduction in the SiC content in the Mg_8 sample [16]. Additionally, impurities introduced by the Mg additives also impact the SiC content in the final product. The composition of the formed SiC and the associated impurities can be more clearly identified using the XRD analysis.

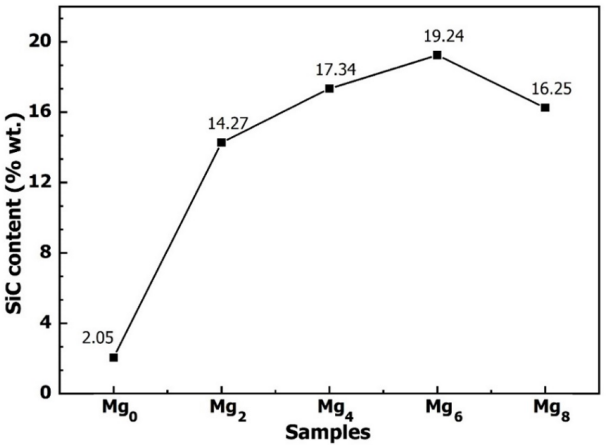

Figure 2. The SiC content of the samples after sintering at 1000 °C.

Figure 3 presents the XRD patterns of the product after sintering at 1000 °C, indicating the presence of various mineral phases. The identified phases include cristobalite (JCPDS Card No. 01-082-1554), α-SiC (JCPDS Card No. 01-073-1664), β-SiC (JCPDS Card No. 29-1129), magnesium (Mg, JCPDS Card No. 35-0821), magnesium oxide (MgO, JCPDS Card No. 78-0430), magnesium silicide (Mg_2Si, JCPDS Card No. 35-0773), and forsterite (Mg_2SiO_4, JCPDS Card No. 34-0189) [17-24]. These minerals are crucial for assessing the structural and chemical properties of the material post-sintering.

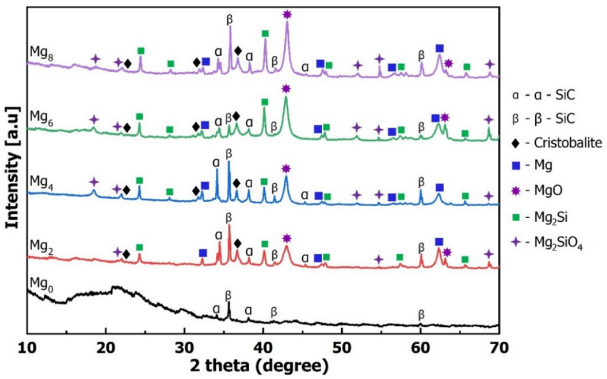

Figure 3. The XRD patterns of the samples after sintering at 1000 °C.

The mineral phases detected in the sample without Mg additives (Mg_0) included cristobalite, α-SiC, and β-SiC. Cristobalite is a form of SiO_2 commonly formed when rice husks are pyrolysed at temperatures above 500 °C. Additionally, cristobalite was produced from the dehydration of silica gel. SiO_2, particularly in the form of cristobalite, is an unavoidable impurity when synthesising SiC from biomass materials such as rice husks [25]. Both α-SiC (high-temperature phase) and β-SiC (low-temperature phase) were detected,

indicating the presence of multiple SiC allotropes in the product. This suggests that the sintering process at 1000 °C is effective not only for the formation of β-SiC, but also for the production of α-SiC, which typically forms at higher temperatures. Furthermore, the broad diffraction band from 10° to 30° shows that the sample, after sintering, still contains amorphous carbon. Amorphous carbon is also considered an impurity in studies involving the SiC synthesis of a biomass [25].

In the samples containing Mg additives, the presence of cristobalite, α-SiC, and β-SiC phases was similar to that observed in the Mg_0 sample. However, a notable difference was observed in the intensity of the diffraction peaks. The peaks corresponding to α-SiC and β-SiC were more pronounced in the Mg-added samples compared to the Mg_0 sample, suggesting that the presence of Mg facilitated the formation of SiC. This finding aligns with previous studies, demonstrating that Mg can act as a catalyst, enhancing the SiC formation and improving its crystallinity [26]. These results also correlate with those presented in Figure 2, where Mg additives were shown to play a critical role in increasing the overall SiC content.

In addition to SiC and cristobalite, the samples with Mg additives also exhibited diffraction peaks corresponding to metallic Mg, MgO, Mg_2Si, and Mg_2SiO_4. These peaks were absent in the Mg_0 sample, confirming that the presence of Mg in the raw material led to the formation of magnesium oxide compounds during the sintering process. These compounds likely formed due to the oxidation of Mg at high temperatures. While Mg contributes positively by promoting SiC formation, it also introduces impurities such as Mg, MgO, Mg_2Si, and Mg_2SiO_4, which can impact the quality of the SiC if not adequately controlled.

The formation of SiC, magnesium oxides, and cristobalite indicates that the Mg additive has a dual effect. It not only enhances the SiC synthesis, but also introduces unwanted impurities. Overall, the XRD analysis offers valuable insights into the structure and composition of the product, confirming that using Mg as an additive in the synthesis of SiC from biomass holds significant potential to improve the production efficiency. However, the careful management of the introduced impurities also necessitates it. The presence of these impurities is not entirely detrimental, as they can be controlled or removed in subsequent processing steps. In this case, an HF acid treatment was employed to eliminate some impurities.

Figure 4 illustrates the results of the SiC content analysis for the samples treated with acid, neutralised with NaOH, and subsequently washed with distilled water. The data presented in Figure 4 highlight the changes in the SiC content following the impurity removal, particularly in the samples with the Mg additives. Notably, the SiC content exhibited a marked increase when transitioning from the sample without additives (Mg_0) to the sample with additives (Mg_2). This trend continued with the increasing additive concentration in the Mg_6 sample. However, when the additive ratio reached an RH/Mg of 1/8 in the Mg8 sample, the increase in the SiC content became minimal, increasing only from 84.25 to 86.15 % by weight. This suggests that the excessive addition of additives does not significantly enhance the SiC content and may even increase impurities in the product, thereby elevating the costs associated with the impurity treatment.

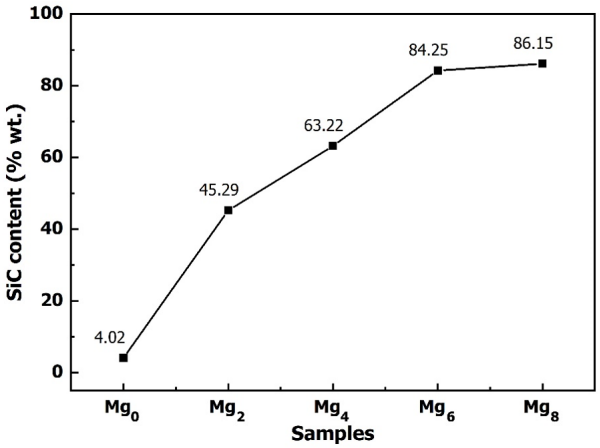

Figure 4. The SiC content of the samples after treatment with the HF acid solution.

Notably, in the Mg_0 sample without additives, the SiC content before and after treatment increased from 2.05 to 4.02 % by weight, indicating a relatively low level of SiC formation. In contrast, the SiC content in the samples with the additives increased sharply, ranging from 14.27 to 19.24 % prior to treatment and from 45.29 to 86.15 % following the treatment. This difference underscores the crucial role of the Mg additive in facilitating the SiC formation process and enhancing the reaction efficiency. Figure 2 also illustrates that the difference in the SiC content between the samples with and without additives before the impurity removal was approximately 17.19 % by weight. However, after the impurities were removed using the acid treatment method (as shown in Figure 4), the difference in the SiC content significantly increased, exceeding 86.15 % by weight. This confirms that the primary impurities in the product are magnesium compounds, and their removal can substantially enhance the SiC content of the final product.

The primary impurities in the additive samples are predominantly related to the magnesium compounds, including Mg, MgO, Mg_2Si, and Mg_2SiO_4. The observed decrease in the SiC content in the Mg_8 sample, as shown in Figure 2, may be attributed to these magnesium compounds, which could adversely affect the SiC formation process or lower the SiC yield. Therefore, optimising the amount of Mg additive is essential to balance the efficiency of the SiC formation and the control of impurities. The results indicated that,

under the experimental conditions, the Mg additive amount in the Mg_6 sample was optimal for achieving the highest efficiency in the SiC formation. The mineral composition following the acid treatment was further analysed using X-ray diffraction.

Figure 5 presents the results of the XRD analysis for the samples after sintering at 1000 °C and subsequent treatment with the HF acid solution. The X-ray diffraction patterns shown in Figure 5 provide evidence of impurity removal following the acid treatment and enable the accurate identification of the remaining crystalline phases in the product. Before treatment, the samples exhibited peaks corresponding to cristobalite, Mg, MgO, Mg_2Si, and Mg_2SiO_4. However, after the HF acid treatment, these peaks were utterly absent, indicating the effective removal of the metallic and oxide impurities.

In particular, removing the MgO peaks facilitated the clear identification of the α-SiC and β-SiC allotropes. This distinction is significant as it indicates that the purification process has eliminated factors that could obscure the accurate determination of the crystal structures of SiC. The chemical reactions (1) to (5) are essential for breaking bonds and removing the impurity compounds, resulting in a purer product. The analytical results demonstrate that the final product after treatment predominantly consists of SiC in the forms of α-SiC and β-SiC, which are highly valuable allotropes in industrial applications due to their superior mechanical and thermal properties. However, a small quantity of free carbon remains in the sample, likely resulting from the incomplete removal of carbon compounds during treatment. The presence of free carbon is evident in the XRD pattern of the Mg_0 sample in Figure 5 within the diffraction range of 10° to 30°. This suggests that the purification process could be further optimised to achieve a product of even higher purity.

$$SiO_2 + 4HF \rightarrow SiF_4 + 2H_2O \quad (1)$$

$$Mg + 2HF \rightarrow MgF_2 + H_2\uparrow \quad (2)$$

$$MgO + 2HF \rightarrow MgF_2 + H_2O \quad (3)$$

$$Mg_2Si + HF \rightarrow MgF_2 + SiF_4 + H_2\uparrow \quad (4)$$

$$Mg_2SiO_4 + 4HF \rightarrow 2MgF_2 + H_4SiO_4 \quad (5)$$

The SEM was employed to observe the mineral formation before and after the acid treatment. Figure 6 displays the SEM images of the samples: (a) the Mg_0 samples before treatment, (b) the Mg_6 samples before treatment, and (c) the Mg_6 samples after treatment with the HF acid solution.

The SEM images of the Mg_0 sample (Figure 6a) reveal that characteristic crystals of α-SiC and β-SiC are formed even without additives, consistent with findings from previous studies [27-29]. This indicates the feasibility of successfully synthesising SiC at low temperatures using the appropriate technology. In addition to SiC crystals, porous frameworks are visible. These

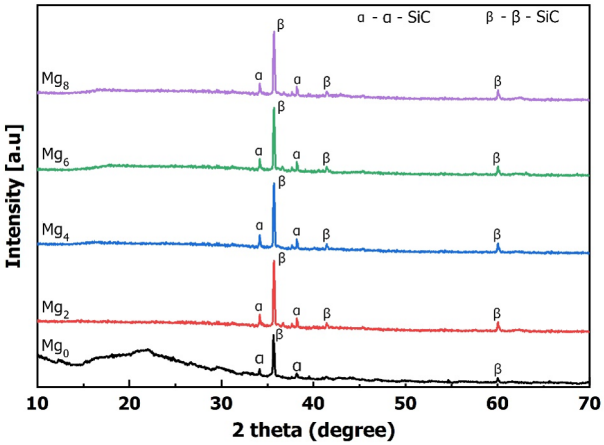

Figure 5. The XRD patterns of the samples after treatment with the HF acid solution.

frameworks represent the residue from the hydrocarbon structure of cellulose, identified as the skeleton of rice husk ash (SRH in Figure 6a), formed during the thermal decomposition process. According to the published literature, this porous framework primarily consists of amorphous carbon generated during the decomposition of cellulose at elevated temperatures. The presence of carbon skeletons suggests that, in the absence of additives, the reaction efficiency between carbon (C) and silicon (Si) to form SiC is relatively low. Consequently, a significant amount of free carbon remains in the sample, indicating the incomplete SiC synthesis and the need for an improved reaction efficiency. Additionally, the presence of these porous carbon skeletons may influence the properties and structure of the final product. This implies that optimising the reaction conditions - such as incorporating additives or implementing a tighter temperature control - could significantly enhance the quality and yield of the SiC synthesis.

Compared to the SEM image of the Mg_0 sample in Figure 6a, the SEM image in Figure 6b does not display the presence of carbon skeleton structures. This absence indicates that the Mg additive has positively influenced the formation of SiC. Specifically, the presence of Mg significantly reduces the amount of free carbon in the sample, thereby enhancing the effectiveness of the SiC formation process. When Mg melts, the surface tension draws the Si and C atoms closer, facilitating their reaction. In addition to SiC crystals, impurities such as MgO, Mg_2Si, and Mg_2SiO_4 are also clearly visible in the SEM images of the samples [30-32]. The SEM images further demonstrate that MgO, Mg_2Si, and Mg_2SiO_4 frequently coexist in the same regions, suggesting that these impurities may arise from the oxidation of Mg and its reaction with Si during heat treatment. Although these impurities can affect the purity of the SiC product, they also provide valuable insights into the reaction environment and the interactions among components within the sample.

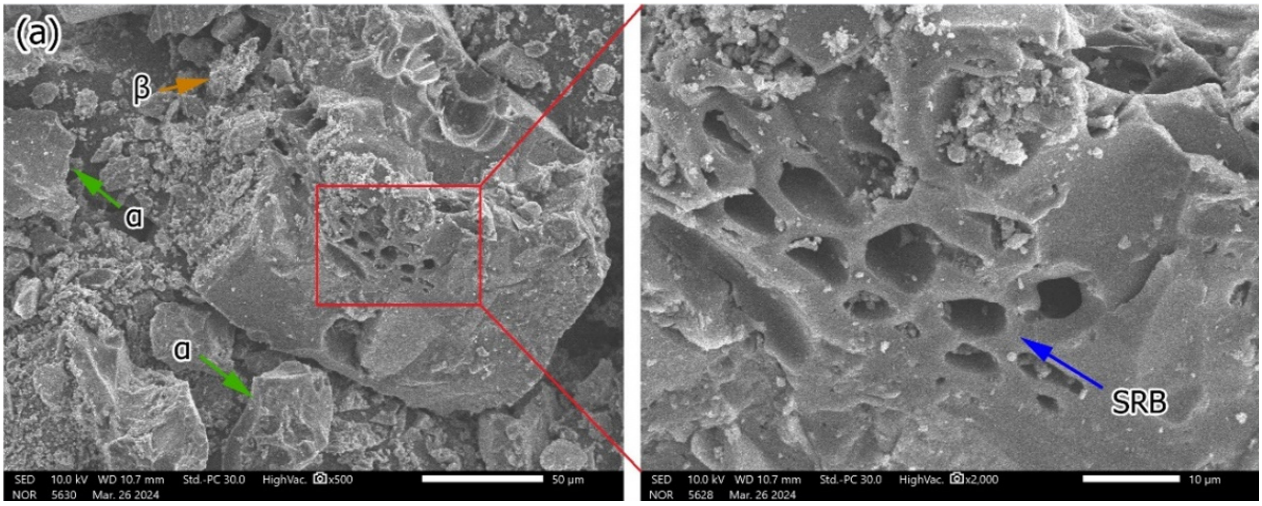

a) the Mg_0 samples before treatment

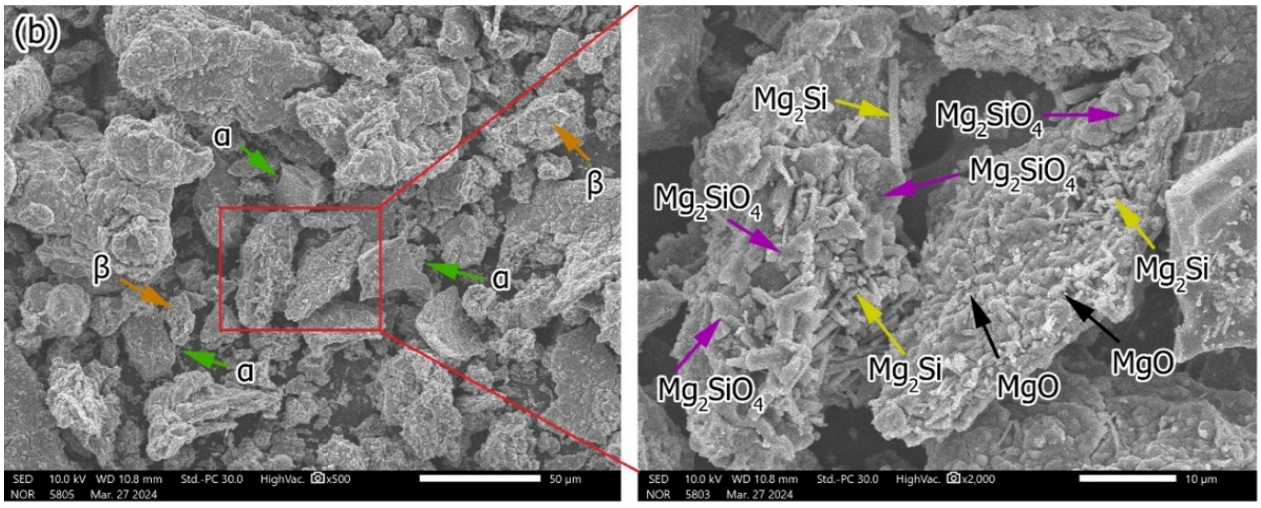

b) the Mg_6 samples before treatment

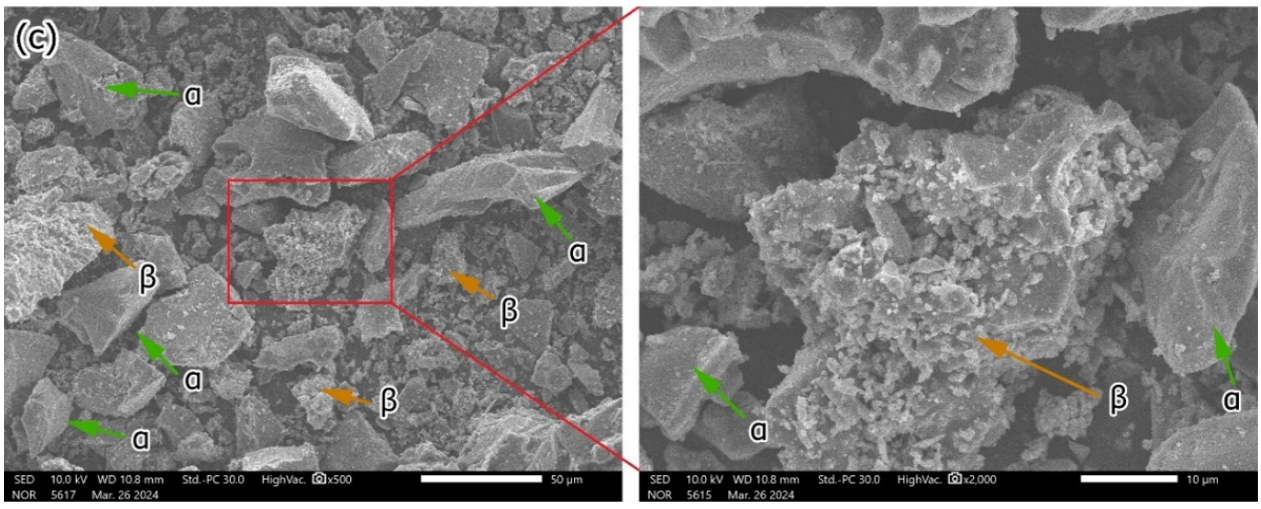

c) the Mg_6 after treatment with the HF acid solution

Figure 6. The SEM of the samples.

Impurities such as MgO, Mg_2Si, and Mg_2SiO_4 are no longer present in Figure 6c, further confirming the effectiveness of the HF treatment on the product. Following the HF treatment, these impurities are removed, resulting in a denser arrangement of α-SiC and β-SiC crystals. The contrast in crystal density of α-SiC and β-SiC between Figure 6a and 6c also indicates that the Mg additive enhances the reaction

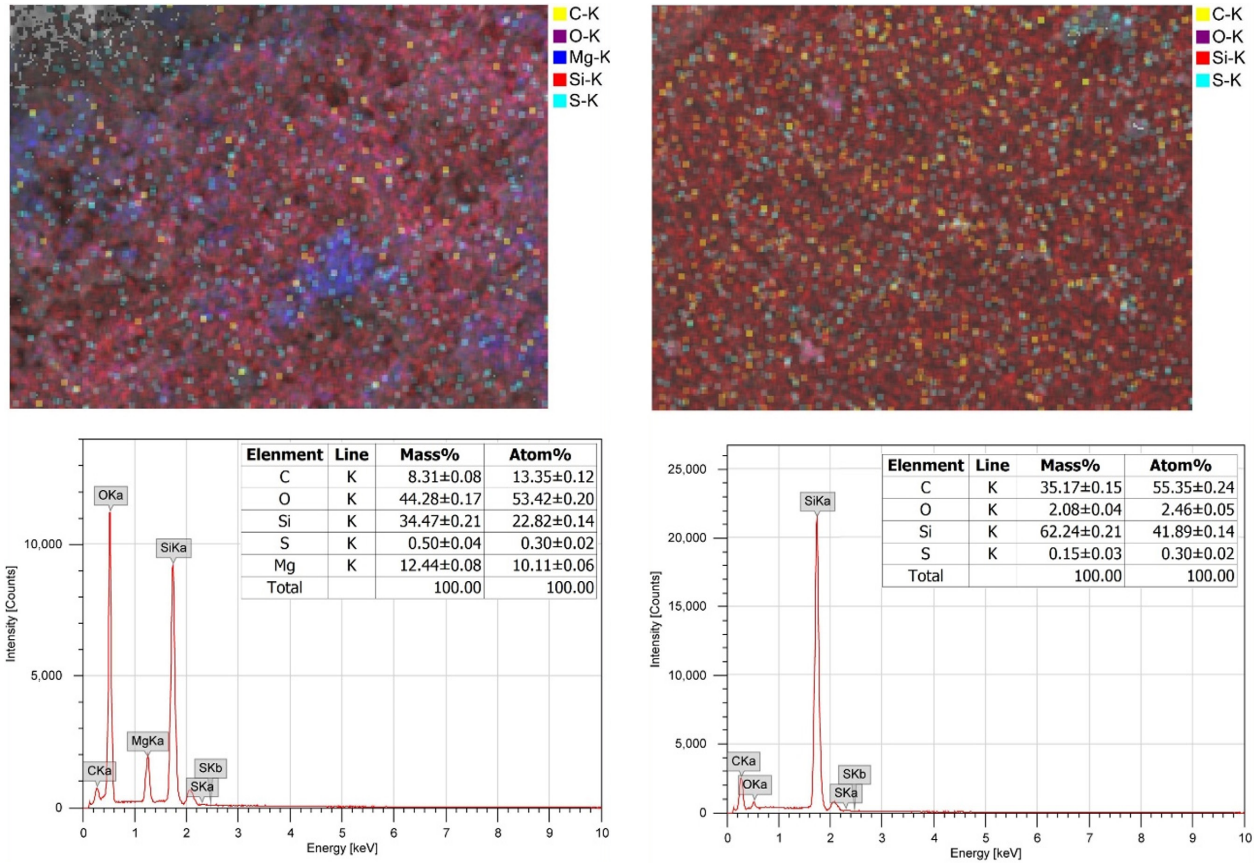

a) before treatment b) after treatment

Figure 7. The EDX results of the samples before and after treatment with the HF acid solution.

and improves the distribution and structure of SiC within the product. Furthermore, the differences between the samples before and after the acid treatment are clearly illustrated in the EDX analysis results shown in Figure 7.

Figure 7 presents the EDX analysis results of the Mg_6 sample before and after the acid treatment. The analysis indicates that the primary elements in the sample are carbon (C), oxygen (O), and silicon (Si), with minor elements including sulfur (S) and magnesium (Mg). C, O, and Si presence corresponds to SiC, SiO_2, and amorphous carbon minerals. In the sample before the acid treatment, detecting elemental components such as Si, Mg, C, and O indicates that SiC, SiO_2, Mg, and amorphous carbon are the main constituents. Conversely, the acid-treated sample exhibited a significant reduction in the oxygen content and the absence of Mg, confirming that the primary mineral components are SiC and amorphous carbon. This further validates the effectiveness of the acid treatment process in removing Mg and SiO_2 compounds from the product.

CONCLUSIONS

This study elucidates the influence of the Mg additive content on the synthesis of SiC from rice husk and silica gel at a sintering temperature of 1000 °C in a CO_2 atmosphere. The results indicate that the presence of Mg significantly affects the formation of SiC. However, the resulting product still contains various impurities, including free carbon, cristobalite, Mg, MgO, $MgSi_2$, and Mg_2SiO_4. Most of these impurities can be effectively removed through treatment with an HF acid solution. Analysis using techniques, such as the SiC content determination, XRD, and SEM/EDX before and after treatment, demonstrated that the impurities were nearly completely eliminated. Notably, the sample with a rice husk to Mg ratio of 1/6 was found to be optimal, achieving an SiC content of up to 84.25 % by weight. The processed product predominantly consists of SiC in its two allotropic forms, α-SiC and β-SiC, along with a minor amount of free carbon. The findings suggest that SiC products derived from rice husks with a high SiC content can be used to manufacture wear-resistant and heat-resistant products.

Acknowledgments

This research is funded by the Vietnam National University Ho Chi Minh City (VNU-HCM) under grant number: B2023-20-18. We acknowledge Ho Chi Minh City University of Technology (HCMUT), VNU-HCM for supporting this study.

REFERENCES

1. Kien K.D.T, Thuy N.C., Minh H.N. (2024): Effect of temperature on the ability to synthesize SiC from rice husks. *Materials Research Express, 11*, 055510. doi: 10.1088/2053-1591/ad4981
2. Salman S.M., Salama S.N. (2011): Crystallization and thermal expansion characteristics of In_2O_3 – containing lithium iron silicate – diopside glasses, *Ceramic-Silikáty, 55*, 114-122.
3. Via F.L., Alquier D., Giannazzo F., Kimoto T., Neudeck P., Ou H., Roncaglia A., Saddow S.E., Tudisco S. (2023): Emerging SiC applications beyond power electronic devices. *Micromachines, 14*, 1200. doi: 10.3390/mi14061200
4. Xun Q., Xun B., Li Z., Wang P., Cai Z. (2017): Application of SiC power electronic devices in secondary power source for aircraft. *Renewable and Sustainable Energy Reviews, 70*, 1336-1342. doi: 10.1016/j.rser.2016.12.035
5. Alweendo S.T., Johnson O.T., Shongwe M.B., Kavishe F.P., Borode J.O. (2019): Synthesis, optimization and characterization of silicon carbide (SiC) from rice husk. *Procedia Manufacturing, 35*, 962-967. doi: 10.1016/j.promfg.2019.06.042
6. Lundqvist D. (1948): On the crystal structure of silicon carbide and its content of impurities. *Acta Chemica Scandinavica, 2*, 177.
7. Liang H., Lu J., Yan Q., Song T. (2018): Chemical catalysts of Fenton reaction for single-crystal SiC based on nanoindentation. I*nternational Journal of Abrasive Technology, 8*, 232-244. doi: 10.1504/ijat.2018.094171
8. Dong S., Zhang X., Hu P., Zhang W., Han J., Hu P. (2019): Biomass-derived carbon and polypyrrole addition on SiC whiskers for enhancement of electromagnetic wave absorption. *Chemical Engineering Journal, 359*, 882-893. doi: 10.1016/j.cej.2018.11.101
9. Krishnarao R., Godkhindi M. (1992): Distribution of silica in rice husks and its effect on the formation of silicon carbide. *Ceramics International, 18*, 243-249. doi: 10.1016/0272-8842(92)90102-J
10. Krishnarao R.V. (1995): Effect of cobalt catalyst on the formation of SiC from rice husk silica-carbon black mixture. *Journal of Materials Science, 30*, 3645-3651. doi: 10.1007/BF00351879
11. Lodhe M., Selvam A., Udayakumar A., Balasubramanian M. (2016): Effect of polycarbosilane addition to a mixture of rice husk and coconut shell on SiC whisker growth. *Ceramics International, 42*, 2393-2401. doi: 10.1016/j.ceramint.2015.10.037
12. Wang F., Qin X., Zhu D., Meng Y., Yang L., Sun L., Ming Y. (2015): FeCl2-assisted synthesis and photoluminescence of *β*-SiC nanowires. *Materials Science in Semiconductor Processing, 29*, 155-160. doi: 10.1016/j.mssp.2014.02.007
13. Shi Y., Zhang F., Hu Y.S., Sun X., Zhang Y., Lee H.I., Chen L., Stucky G.D. (2010): Low-temperature pseudomorphic transformation of ordered hierarchical macro-mesoporous SiO_2/C nanocomposite to SiC via magnesiothermic reduction. *Journal of the American Chemical Society, 132*, 5552-5553. doi: 10.1021/ja1001136
14. Romero F.N., Reinoso F.R. (1996): Synthesis of SiC from rice husks catalysed by iron, cobalt or nickel. *Journal of Materials Science, 31*, 779-784. doi: 10.1007/BF00367899
15. Hai L.V, Nhan H.T.C., Huy H.T. (2013): Synthesis of silica nanoparticles from Vietnamese rice husk by sol–gel method. *Nanoscale Research Letters, 8*, 1-10. doi: 10.1186/1556-276X-8-58
16. Sun L., Gong K. (2001): Silicon-based materials from rice husks and their applications. *Industrial & Engineering Chemistry Research, 40*, 5861-5877. doi: 10.1021/ie010284b
17. Elzea J., Odom I., Miles W. (1994): Distinguishing well ordered opal-CT and opal-C from high temperature cristobalite by x-ray diffraction. A*nalytica Chimica Acta, 286*, 107-116. doi: 10.1016/0003-2670(94)80182-7
18. Noviyanto A., Wibowo A., Sukmarani G., Kusumaningrum R., Fauzi F., Habieb A.M., Amal M.I., Rochman N.T. (2020): Ceramic composites derived from polysilazane with the addition of silicon carbide. *Journal of Ceramic Processing Research, 21*, 326-330. doi: 10.36410/jcpr.2020.21.3.326
19. Lin X., Xu Q., Deng T., Yang B., Chen L. (2024): Improving thermal conductivity of Al/SiC composites by post-oxidization of reaction-bonded silicon carbide preforms. *Scientific Reports, 14*, 16610. doi: 10.1038/s41598-024-67653-y
20. Zhu D., Gao M., Pan H., Pan Y., Liu Y., Li S., Ge H., Fang N. (2014): Fabrication and mechanical properties of SiCw (p)/SiC-Si composites by liquid Si infiltration using pyrolysed rice husks and SiC powders as precursors. *BioResources, 9,* 2572-2583. doi: 10.15376/biores.9.2.2572-2583
21. Yi J. Xue W.J., Xie Z.P., Liu W., Cheng L.X., Chen J., Wang L., Cheng H., Gao Y.X., Wang H.B. (2013): The dependence of interlocking and laminated microstructure on toughness and hardness of *β*-SiC ceramics sintered at low temperature. *Materials Science and Engineering: A, 586*, 338-341. doi: 10.1016/j.msea.2013.08.033
22. Abrinaei F. (2017): Nonlinear optical response of Mg/MgO structures prepared by laser ablation method. *Journal of the European Optical Society-Rapid Publications, 13*, 15. doi: 10.1186/s41476-017-0042-z
23. Yi Z., Shan Z., Fang L., Lu C., Xu Z. (2023): Enhanced photostability of chlorophyll by introducing Mg_2Si as an O_2-depleting agent. *Journal of Materials Science, 58*, 6281-6296. doi: 10.1007/s10853-023-08398-3
24. Yan X., Liu Y., Tang C., Liu S., Ge W., Tong J., Meng F. (2022): Microwave dielectric properties of Mg_2SiO_4–$Ca_{1-y}Sm_{2y}/3TiO_3$ composite ceramics. *Journal of Materials Science: Materials in Electronics, 33*, 19751-19758. doi: 10.1007/s10854-022-08757-x
25. Tang Q., Chen X., Zhou D., Liu C. (2021): Biomass-derived hierarchical porous carbon/silicon carbide composite for electrochemical supercapacitor. *Colloids and Surfaces A: Physicochemical and Engineering Aspects, 620*, 126567. doi: 10.1016/j.colsurfa.2021.126567
26. Raju K., Yoon D.H. (2016): Sintering additives for SiC based on the reactivity: a review, *Ceramics International, 42*, 17947-17962. doi: 10.1016/j.ceramint.2016.09.022

27. Baitalik S., Kayal N., Dey A., Chakrabarti O. (2014): Effect of SiC particle size on the material and mechanical properties of mullite bonded SiC ceramics processed by infiltration technique. *Ceramics-Silikáty, 58*, 326-332.
28. Jain V.K.S., Muthukumaran S. (2019): Influence of SiC content on microstructure and tribological properties of friction stir-processed SiC/AA5083 surface composites. *Metallurgical and Materials Transactions A, 50*, 2933-2944. doi: 10.1007/s11661-019-05219-8
29. Liu B., Yang J. (2020): Fabrication of highly dense pure 6H-SiC ceramics via the PVT methodusing sub-micro SiC powders. *Ceramics-Silikáty, 64*, 135-144. doi: 10.13168/cs.2020.0002
30. Ding Y.D., Song G., Zhu X., Chen R., Liao Q. (2015): Synthesizing MgO with a high specific surface for carbon dioxide adsorption. *RSC Advances, 5*, 30929-30935. doi: 10.1039/C4RA15127E
31. Tebib M., Samuel A., Ajersch F., Chen X.G. (2014): Effect of P and Sr additions on the microstructure of hypereutectic Al–15Si–14Mg–4Cu alloy. *Materials Characterization, 89,* 112-123. doi: 10.1016/j.matchar.2014.01.005
32. Tang C., Liu Y., Yan X., Liu S., Ge W., Tong J., Meng F. (2022): Phase composition, crystal structure, and microwave dielectric properties of $0.8Mg_2SiO_4$–$0.2Ca_{0.9}Sm_{0.2}/3Al_{4x}/3Ti_{1-x}O_3$ ceramics. *Journal of Materials Science: Materials in Electronics, 33*, 22119-22126. doi: 10.1007/s10854-022-08981-5